

MORE: Simultaneous Multi-View 3D Object Recognition and Pose Estimation

Tommaso Parisotto, Hamidreza Kasaei

Abstract—Simultaneous object recognition and pose estimation are two key functionalities for robots to safely interact with humans as well as environments. Although both object recognition and pose estimation use visual input, most state-of-the-art tackles them as two separate problems since the former needs a view-invariant representation while object pose estimation necessitates a view-dependent description. Nowadays, multi-view Convolutional Neural Network (MVCNN) approaches show state-of-the-art classification performance. Although MVCNN object recognition has been widely explored, there has been very little research on multi-view object pose estimation methods, and even less on addressing these two problems simultaneously. The pose of virtual cameras in MVCNN methods is often pre-defined in advance, leading to bound the application of such approaches. In this paper, we propose an approach capable of handling object recognition and pose estimation simultaneously. In particular, we develop a deep object-agnostic entropy estimation model, capable of predicting the best viewpoints of a given 3D object. The obtained views of the object are then fed to the network to simultaneously predict the pose and category label of the target object. Experimental results showed that the views obtained from such positions are descriptive enough to achieve good accuracy score. Code is available online at: https://github.com/tParisotto/more_mvcnn

I. INTRODUCTION

Nowadays, robots are leaving pre-defined setting and helping humans in many collaborative tasks in both industrial and human-centric environments. In order to safely interact with users and environments, robots need to recognize a range of objects and estimate their poses precisely from different perspectives. It is a challenging task due to high demand for accurate object recognition and precise pose estimation, as the output of these tasks will be used as input for the purpose of object manipulation. For instance, consider the task of serving a coke can: the robot first needs to know which type of objects exist in the scene, where they are, and then grasp and manipulate the can on top of the mug and the pour the coke into the mug. Although object recognition and pose estimation tasks both require visual information as input, they are often contradicting from a problem definition point of view. In particular, a robot needs to learn pose-invariant features of objects to be able to recognize them accurately from different viewpoints; In contrast, the robot requires to learn pose-dependent features of objects to be

Department of Artificial Intelligence, Bernoulli Institute, University of Groningen, 9747 AG, The Netherlands. Email: t.parisotto@student.rug.nl hamidreza.kasaei@rug.nl

We thank NVIDIA Corporation for their generous donation of GPUs which was partially used in this research.

able to estimate their pose. This is the main reason that state-of-the-art approaches address object recognition and pose estimation often as two separate problems. Recent multi-view deep learning approaches achieved the best results in both object recognition and pose estimation, when they tackled these problem separately. The pose of virtual cameras in MVCNN methods is often pre-defined in advance, leading to limitations in the application of such approaches.

Although many problems have already been understood and solved successfully, many challenges still remain. Simultaneous object recognition and pose estimation is one of the challenges waiting for many improvements. In this paper, we are taking a step towards addressing this problem. Specifically, we propose a multi-view deep learning approach to handle object recognition and pose estimation simultaneously by sharing representations between these tasks. In particular, we develop a deep object-agnostic entropy estimation model, capable of predicting the most informative viewpoints of a given 3D object. The obtained views of the object are then fed to the network to simultaneously predict the pose and category label of the target object. An illustrative overview of the proposed approach is shown in Fig. 1.

II. RELATED WORK

Three-dimensional (3D) object recognition and pose estimation have been under investigation for a long time in both computer vision and robotics communities. Although an exhaustive survey of recent deep learning based approaches is beyond the scope of this paper, we will review the main efforts.

There are substantially three main approaches for CNN-based object recognition: volume-based, point-based, and view-based approaches. Volume-based approaches use volumetric representation of data, in particular they employ voxels to obtain a discrete representation of objects and define a data structure. These networks learn features from the occupancy grids which represent the objects in space. Point-based approaches are popular with data retrieved with 2.5D depth sensors. These sensors capture a dense set of depth samples from the scene, representing the surface of the objects as a collection of points in the Euclidean space. Point-based neural networks learn features about the positional relations between points on the surfaces of objects. View-based approaches use one or more images representations of the objects, usually captured with a camera from a specific viewpoint. CNNs trained on such representations learn features from the visible

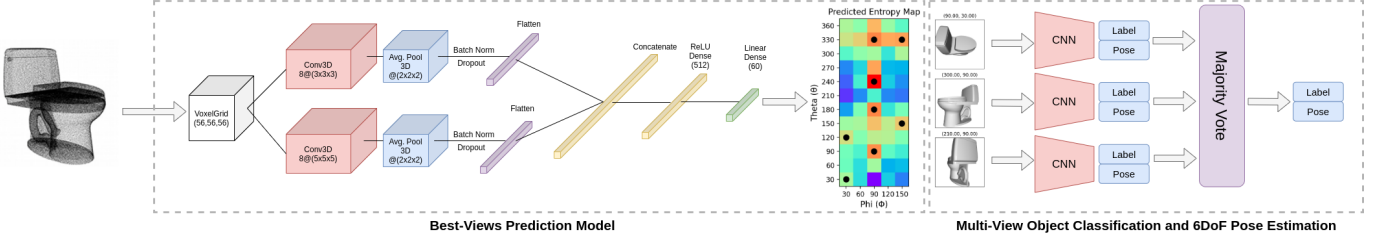


Fig. 1. The 3D object is transformed into a $56 \times 56 \times 56$ voxel grid which is the input size for our model. The entropy model uses a branching architecture that converges into a fully connected layer. The output of the entropy model is a 60-values vector which is reshaped into a 2D entropy map. From the entropy map a peak selection algorithm returns the coordinates of the local maxima. We extract the views corresponding to those coordinates and we use them as input for as many CNNs. The label and pose predictions are pooled by majority vote, resulting in the final prediction.

attributes of the objects. The availability of 3D data usually induces to directly apply recognition algorithms on a three-dimensional representation of that data, however, it has been shown that view-based methods outperformed other methods and achieved better performance.

Qi et al. [1] provides a comprehensive study on voxel-based CNNs and multi-view CNNs for three dimensional object classification, stating that empirical results from the view-based and volume-based types of CNNs exhibit a large gap, indicating that existing volumetric CNN architectures and approaches are unable to fully exploit the power of 3D representations. Among voxel-based systems, the earliest work would be 3D ShapeNets [2] which developed a Convolutional Deep Belief Network to learn probability distributions of binary occupancy grids. VoxNet [3] designed to tackle object recognition by integrating the voxel representation to deal with large amounts of point cloud data. FPNN [4] employed field probing filters to efficiently extract features from voxel data. 3D-GAN [5] implemented Generative Adversarial Networks (GAN) to generate 3D objects from a probabilistic space and obtain a object descriptor from an adversarial discriminator.

Recent approaches showed that it is possible to achieve significant improvements in classification accuracy by using collections of rendered views of 3D objects [6], [7]. Su et al., [6] obtained object's views by retrieving 2D projections of the object with a set of virtual cameras positioned in a regular setup. The authors opted for a fixed number of virtual camera points, positioning of the cameras on a regular structure around the objects. They demonstrated that a convolutional neural network, trained on a fixed set of rendered views of a 3D shape, could outperform most architectures trained on three-dimensional structured data. It was shown that in many cases a single view already achieves satisfying classification accuracy. Kanezaki et al. proposed a multi-view CNN based approach namely RotationNet [7], which achieved the best state-of-the-art results. They proposed a CNN-based model which takes multi-views images as input and jointly estimates its pose and object category. Viewpoint labels are learned in an unsupervised manner during the training and the architecture is designed to use only a partial set of views for inference. Unlike MVCNN, their method is able to classify an object using a partial set of images that may be sequentially observed

by a moving camera. The system infers the probability of a retrieved view to match the camera position it has been taken from, subsequently determining the orientation of the object.

Joint learning of object classification and pose estimation has already been unraveled by several researches [8]–[11], however, very few of them address inter-class features learning for pose alignment. It has been proved beneficial to share appearance information across classes to simultaneously solve for object classification and pose estimation [12]. Elhoseiny et al. [13] studied CNNs for joint object classification and pose estimation based on multi-view images, discussing architectures of the following archetypes: Parallel Model (PM) consisting of two base networks running in parallel; Cross-Product Model (CPM) explores a way to combine categorization and pose estimation by building a last layer capable of capturing both; Late Branching Model (LBM) splits the network into two last layers, each designed to be specific to the two tasks; Early Branching Model (EBM) is similar to LBM, however the branching is moved to an earlier layer in the network. While their method takes a single image as input for its prediction, later works focused on how to aggregate predictions from multiple images captured from different viewpoints [7].

The best-view selection corresponds to the automated task of selecting the most representative view of a 3D model. Dutagaci et al. [14] provides a benchmark for the evaluation of best-view algorithms and a survey on popular methods of best-view selection. The algorithms discussed by Dutagaci et al. differ with respect to the descriptor they use to assess the goodness of a view, which are assumed to measure the geometric complexity of the visible surface of an object.

III. METHODS

We propose a deep learning approach to infer the best-views of a 3D model, which uses the obtained views to perform both object recognition and pose estimation tasks. We subdivide the problem in two main tasks, the first being the best-view prediction and the second being the multi-view based object recognition and pose estimation.

A. Best-Views Prediction Model

The main objective is to design a model that predicts which point of views are most informative. In this vein, we first need to define how we measure quantitatively the goodness

of a view. We evaluate the quantity of information for each view by calculating the entropy of depth image captured from the same viewpoint with the definition from Shannon's information theory:

$$H(X) = - \sum_{i=1}^n p(x_i) \log p(x_i), \quad (1)$$

where x_i represents the value of i th pixel [15] [16]. Most measures require a less extensive evaluation of the 3D model, while this method expects to have several projected views of the object in advance which are computationally expensive to obtain. However, our intention is to make use of an object-agnostic CNN model to directly infer the best-views from the 3D model, providing an evaluation of the information about its surfaces with no pre-processing required. Towards this goal, instead of a multi-label classification problem where we classified each viewpoint as informative or not, we defined the problem as a regression to infer the entropy values of every viewpoint, generating a spherical entropy map of the object. The entropy map $H(\phi, \theta)$ is learned in the form of a 2D function that maps two spherical coordinates, ϕ and θ necessary to identify the viewpoints on a sphere around the object to the inferred entropy values: $H : (\phi, \theta) \rightarrow h$. The coordinates of the most informative views are then obtained by evaluating the peaks of the entropy map:

$$\{(\phi_v, \theta_v)\} = \operatorname{argmax}_{\phi, \theta} \left(\frac{d^2 H}{d\phi d\theta} = 0 \right). \quad (2)$$

We design a CNN approach to estimate an entropy map for a given object. As shown in Fig. 1, we employ two convolutional branches with kernels of different sizes separating the flow of the graph from the input layers. Supposedly the different kernel size help the network identifying high level features of different scales. The output of the convolutional branches both receive average pooling, batch normalization and dropout before being transformed into flat vectors. The outputs of the branches are then concatenated in a single vector and sent as input to a fully connected hidden layer. The last layer is a fully connected output layer with linear activation that outputs 60 entropy values (see Figure 1). The optimal number of filters for the convolutional layers and the number of units in the hidden layer was estimated empirically with a hyper-parameters based on the search algorithm Hyperband [17], a bandit-based approach to hyper-parameters optimization that speeds up random search through adaptive resource allocation and early-stopping. It evaluates architectures by training a set of configurations for a limited number of epochs and carrying the evaluation only for the most promising half until it reaches the best set of parameters. We used the Adam optimizer with dynamical learning rate starting at $5e-5$ with reduction on plateau of factor 0.3 and Mean Absolute Error as loss function.

Towards this end, the first step is to generate a dataset taking depth images from a number of views of a collection of objects, in particular we took images from 60 positions, regularly distributed on a sphere. The virtual cameras are

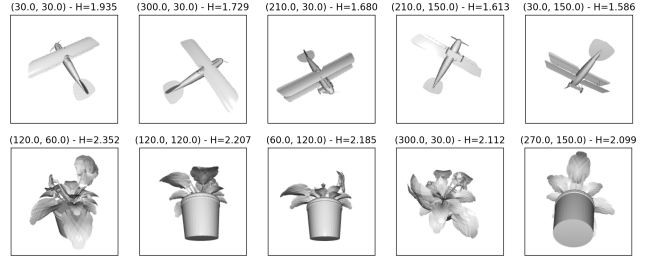


Fig. 2. Five best-views sorted by predicted entropy of unseen object classes: (top) airplane, and (bottom) flower pot.

positioned on 12 points on a section ring of the sphere, each one at an angle of 30 degrees from the next one. The sphere is circled by 5 rings, parallels to the horizontal axis of the object, which are looking at the center of the sphere from each at an angle of 30 degrees from the next one, cutting the sphere at 30, 60, 90, 120 and 150 degrees from the vertical axis of the object. The structure of the camera positions ensures we obtain a complete overview of any object while having a limited number of fixed positions. Once we have the positions for the cameras, we take a grayscale depth image of 224×224 pixels of the object for each of the 60 views. We can then evaluate the quantity of information in each view from calculating their entropy (details are presented in Section IV-A).

We initially trained the model as a best-view classifier, however, such configuration tended to provide a list of best-views based on the most common perspectives for high entropy values instead of learning the relationship between silhouettes and entropy. This issue was due to the unbalance in the training data. We opted for a more efficient solution: we built the dataset by matching each 3D object to its entropy values and trained the 3D-CNN to infer by regression the values from any 3D model. With this solution we observed the network generalises better on new data and it allows for a more precise evaluation of the best-views. Figure 2 shows the five best-views of two never-seen-before objects (*airplane* and *flower pot*) predicted by the proposed model. The obtained views are then used for classification and pose estimation purposes.

B. Multi-View Classification and Pose Estimation

As discussed in the introduction, we aim to design an approach to jointly handle object classification and pose estimation by learning shared high level features. Following the notation from Elhoseiny et al. [13], our design falls in the category of Late Branching Models (LBM). As the backbone of our model, we use an instance of a popular architecture, pre-trained on Imagenet [18], for image recognition, splitting the last layer into two fully connected layers with softmax activation of size 10 and 60 outputs for the object classification and the pose estimation respectively. Particularly, we evaluate MobileNetV2 [19], and VGG-16 [20]. The network was trained as a single-input multiple-outputs model. In particular, the model takes a single-view as an input and it predicts the class of the originating object and the estimated viewpoint.

The multi-view consists in the aggregation of m single-view classifiers where m is the number of views provided for the prediction. This method allows the network to accept a variable number of view images, to then return as outputs the classes represented by the majority votes. While the object labels are quite straightforward to aggregate, different views result in different viewpoints. The predicted viewpoints are matched to the angle the image views they were taken, the offset between these two values is the predicted rotation of the object from a standing front-facing position. Using these values, we can evaluate a majority vote for the pose estimation with precision up to half the distance between each of the 60 originating viewpoints in the dataset (15 degrees on rotation around the z-axis and 15 degrees on rotation around the y-axis). This precision can be utterly improved generating a dataset with a more dense configuration of viewpoints and reshaping the network to classify a larger number of positions, with the cost of increasing the complexity of the network and the number of parameters. As regularization techniques, we used a dynamic learning rate. The learning rate set at the beginning of the training is $1e-4$, it then decreases on plateau by factor 0.5 until reaching a minimum of $1e-8$. This allows the learning process to switch to a progressively finer tuning in the later stages of the training. As loss functions we used categorical cross-entropy for both class and pose prediction.

IV. RESULTS

In this section, we first present the detail of generating a multi-view dataset for training our model and then explain the evaluation metrics. Finally, we discuss the performance of the proposed approach in the case of best-views prediction, single-view, and multi-view object classification and pose estimation.

A. Dataset

To build the dataset for the proposed model, we used the Princeton ModelNet10 dataset [2], which consists in a collection of meshes from 10 popular object categories. To generate depth images from a single 3D object model, virtual cameras are set up to point at the centroid of the object, then 2D depth images are rendered from each camera using a projection method. To achieve a consistent input we scaled each model to fit in a unit cube centered in the origin, we then subdivided the unit cube into a binary voxel grid, in which occupied voxels are shown by 1 and the rest by zero. The obtained binary matrix represents the 3D model silhouette. We experimented with different grid sizes, while a higher number would have increased the resolution of the object, it would have increased exponentially the size of the data. We settled for a grid size of $50 \times 50 \times 50$ which offered an acceptable trade-off between size and resolution. The smoothing effect due to the little details in the object being cut off by the voxelization resolution happened to have a regularization effect in the learning since the convolution layers of the network would not try to learn such details as high-level features. To supply the closeness of the models to the sides of the cube due to the scaling and bounding process, we added a zero-padding

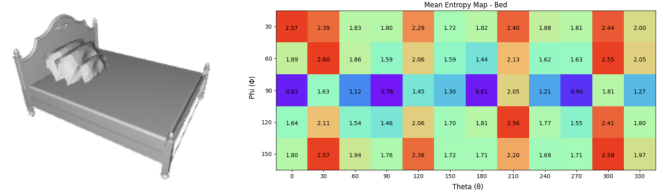


Fig. 3. Average distribution of the 60 views entropy for the class Bed. The coordinates (x, y) of the graph indicate the rotation (θ, ϕ) . θ represents the yaw angle, while ϕ represents the pitch angle.

of three voxels per side resulting in the occupancy grids to be of 56^3 voxels.

We rendered a set of 60 depth images from every object in the ModelNet10 dataset. We evaluated the quantity of information of every image with the Shannon's Entropy (see Eq. 1). To explain the idea better, we provide an example in Fig. 3, representing the average entropy distribution for the category Bed. Given the shape of the average bed, the larger entropy values are found in correspondence to viewpoints closest to the four angles, since such viewpoints frame more faces of the cuboid. It can be seen from the orange-red colours being predominant in the columns relative to the rotation around the z-axis at the values of 30, 120, 210 and 300 degrees. The lowest values instead are found on the row relative to the 90 degrees rotation on the y-axis, meaning the object is being observed frontally. This is the worst angle to observe a cuboid since the upper and lower faces are not visible, hence resulting in the blue-violet row at 90 degrees. We finally built the dataset by matching each 3D object to its entropy values.

B. Evaluation of best-views prediction model

For input voxel grid of size $56 \times 56 \times 56$, we designed two branching 3D convolutional layers with kernels sizes $3 \times 3 \times 3$ and $5 \times 5 \times 5$. The Hyperband algorithm [17] evaluated 8 as the best number of kernels for both the convolutional layers and 512 units for the fully connected layer before the output layer. To accelerate and stabilize the learning process, we applied batch normalization in-between layers, and considered a progressively smaller learning rate (starting at 5×10^{-5} until reaching 3×10^{-7}) and dropout factors of 0.25 on the output of convolution layers and of 0.5 on the fully connected layer. Since we formulate the problem in the form of a multi-output regression with 60 values, the output layer uses a linear activation function and the resulting values are to be intended as entropy values and not probabilities. To evaluate the quality

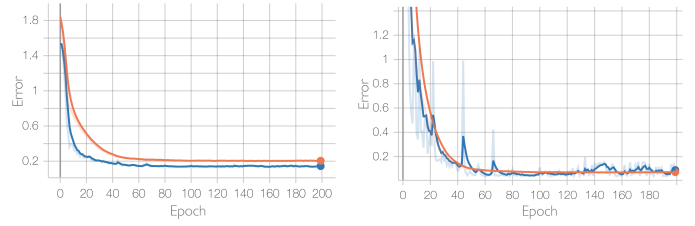


Fig. 4. Training progress of the proposed entropy model on 200 epochs based on (left) MAE and (right) MSE.

of the learning, we used two measures: Mean Absolute Error (MAE) and Mean Squared Error (MSE), the former being employed as the loss function. The resulting learning process is shown in Fig. 4.

It was observed that the network was able to learn a function to approximate the entropy of 60 viewpoints precisely. An example of comparison between the original entropy map (built by calculating entropy of views) and the map predicted by our model for a Toilet object is shown in Fig. 5. The distribution of the predicted values resemble closely the distribution of the true values. To extract the best-views from the entropy map we use a peak detection algorithm that returns the coordinates of the local maxima in the matrices.

C. Evaluation of classification and pose estimation

In this round of experiments, we first evaluated the proposed system using two core architectures, VGG-16 [20] and MobileNetV2 [19], which are reliable CNN architectures for object recognition. Both models are pre-trained using the ImageNet dataset [18], a large dataset consisting of 1.4M images and 1000 classes. The architecture are instantiated without the top layers, to adapt to the branching structure for object classification and pose estimation. The branching is performed at the last layer, following the Late Branching Model (LBM) example by the notation from Elhoseiny et al. [13]. We experimented with different branching archetypes, however the number of parameters increased dramatically without a corresponding improvement in accuracy. The last layer of the core architecture is split in two fully connected layer of size 10 and 60 which represent the number of possible classes and poses. We used the Adam optimizer with a starting learning rate of 1×10^{-4} which is dynamically reduced on plateauing validation loss. As loss functions we employed

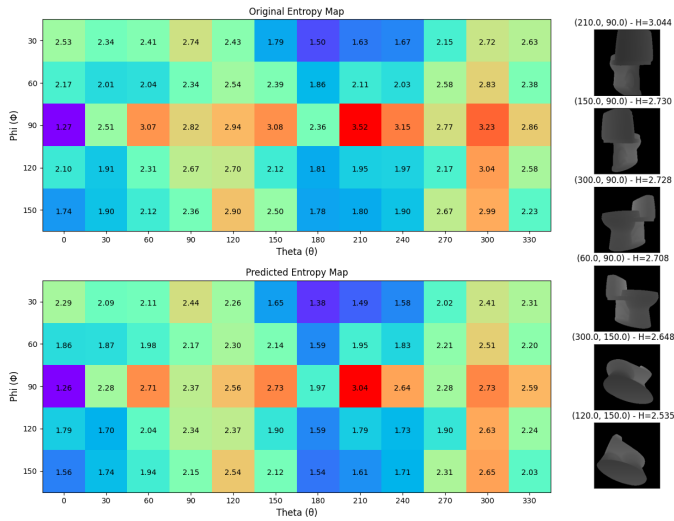


Fig. 5. Entropy map calculated from the projected depth-views of a Toilet class object (top-left) and the map of the same object predicted by our model (bottom-left). The colors indicate the entropy value calculated on a depth-image captured from the position (Θ, Φ) . Violet-blue indicate smaller values while orange-red indicate larger values. The depth images for the six best views in order of entropy are shown on the right.

TABLE I
SINGLE-VIEW OBJECT RECOGNITION AND POSE ESTIMATION ACCURACY.

Model	Sub-sampled Dataset	Class Acc.	Pose Acc.
VGG-16	Full	0.8339	0.7890
VGG-16	1/3	0.8257	0.7972
VGG-16	1/20	0.7807	0.7239
MobileNetV2	Full	0.8459	0.8110
MobileNetV2	1/3	0.8312	0.8092
MobileNetV2	1/20	0.7985	0.7473

categorical cross-entropy for both class and pose. We fine-tuned the architectures on a dataset of 293,940 RGB images of size $224 \times 224 \times 3$, composed of projections from 60 viewpoints of 4,899 3D models from the ModelNet10 dataset. Due to the large amount of data obtained, training the models is a particularly time consuming task. We experimented with random subsets of the full dataset to check whether a fraction of it would achieve similar accuracy while reducing the training time required. The results of training models based on the VGG-16 and MobileNetV2 architectures is summarized in Table I. For each architecture, we tested the accuracy of both networks when trained on the full dataset, on a third (1/3) and a twentieth (1/20) of it. The accuracy metrics describe the ratio of labels, on the test split of the dataset, that are correctly predicted by the model from a single view image. We consider the pose to be correctly predicted when the model reports the coordinates (Θ, Φ) corresponding to the viewpoint used to capture the view.

Our approach bases its final classification and pose estimation on majority vote. Each prediction from the instances of the single-view CNN is pooled and contributes to the decision of the system (see the *right-side* of Fig. 1). We tested the proposed system with the best performing models with architectures based on VGG-16 and MobileNetV2. For a fair comparison we trained the single-view CNN and then tested the proposed approach using the training and test split of the original dataset as in [2], [7]. The accuracy scores are presented in Table II. MobileNetV2 proved to perform better than VGG-16 for the classification of the objects, while the latter showed a slightly improved performance in the estimation of the pose.

We plotted the confusion matrices to show the differences between the prediction of VGG-16 and MobileNet architectures (see Fig. 6). It was observed that both architectures achieved more than 90% accuracy over *bed*, *chair*, *dresser*, *monitor*, *sofa*, and *toilet* classes, and most of misclassifications mainly occurred within the *bathtub*, *desk*, and *night-stand* categories. On closer inspection, we can see that the VGG-16 architecture misclassified *bathtub* with *sofa* more times than MobileNetV2, and also misclassified more frequently a *desk* for other objects. While the overall accuracy on the *desk*

TABLE II
MULTI-VIEW OBJECT RECOGNITION AND POSE ESTIMATION ACCURACY.

Model	Class Accuracy	Pose Accuracy
VGG-16	0.9020	0.9394
MobileNetV2	0.9130	0.9372

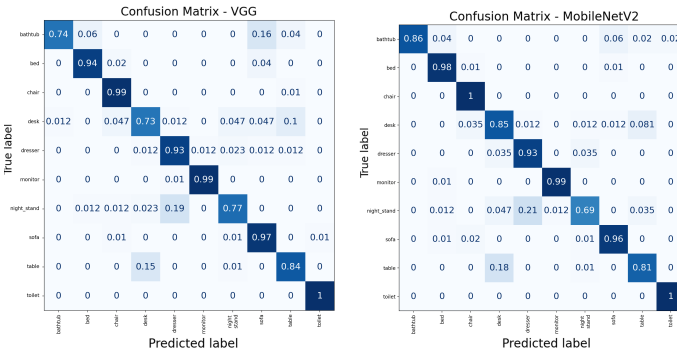


Fig. 6. Confusion matrices for classification with VGG-16 (left) and (right) MobileNetV2 architectures.

class is better for MobileNetV2, VGG-16 is more stable when separating the *table* and *desk* classes which are arguably the most difficult to distinguish. Another difference lies in the classification of the *night-stand* class where VGG-16 performs significantly better than MobileNetV2.

As for the views used by the model to make the predictions, the peak detection algorithm makes the best-view selection and outputs a number of views equal to the number of local maxima in the entropy map. An overview on the distribution of the number of views used for each category is presented in Fig. 7. As it is shown in the graph the model adapts the number of views it uses for the prediction to the supposed complexity of the object it is observing. On average the algorithm selects seven views to perform the prediction.

V. CONCLUSIONS

In this paper, we proposed a deep learning based approach to tackle the simultaneous recognition and pose estimation of 3D objects. We suggested a deep object-agnostic entropy estimation model, capable of predicting the best viewpoints of a given object. We then used the obtained views of the object to predict the pose and category label of the target object simultaneously. Experimental results showed that the predicted views of objects are descriptive enough to achieve high accuracy scores in both classification and pose estimation tasks. In continuation of this work, we would like to further investigate other next-best view prediction metrics to see the possibility of improving both recognition and pose estimation performance. Another potential avenue to look into is a fine pose estimation. In particular, the discrete nature of the

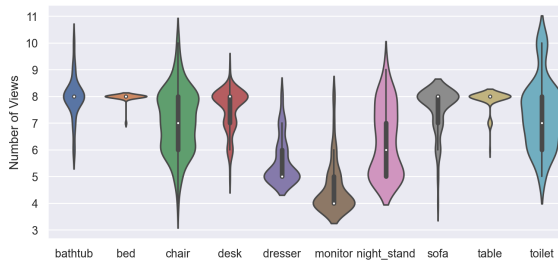


Fig. 7. Violin plot of the distribution of the number of selected best-views for each category from the ModelNet10 dataset.

proposed pose estimation leaves the sensitivity of the pose estimator depending on the density of the dataset, hence it would be possible to achieve more precise estimations by sampling a dataset with a larger number of viewpoints.

REFERENCES

- [1] C. R. Qi, H. Su, M. Nießner, A. Dai, M. Yan, and L. J. Guibas, “Volumetric and multi-view CNNs for object classification on 3D data,” in *Proceedings of the IEEE conference on computer vision and pattern recognition*, 2016, pp. 5648–5656.
- [2] Z. Wu, S. Song, A. Khosla, F. Yu, L. Zhang, X. Tang, and J. Xiao, “3D shapenets: A deep representation for volumetric shapes,” in *Proceedings of the IEEE conference on computer vision and pattern recognition*, 2015, pp. 1912–1920.
- [3] D. Maturana and S. Scherer, “VoxNet: A 3D convolutional neural network for real-time object recognition,” in *2015 IEEE/RSJ International Conference on Intelligent Robots and Systems (IROS)*. IEEE.
- [4] Y. Li, S. Pirk, H. Su, C. R. Qi, and L. J. Guibas, “Fpnn: Field probing neural networks for 3D data,” *arXiv preprint arXiv:1605.06240*, 2016.
- [5] J. Wu, C. Zhang, T. Xue, W. T. Freeman, and J. B. Tenenbaum, “Learning a probabilistic latent space of object shapes via 3D generative-adversarial modeling,” *arXiv preprint arXiv:1610.07584*, 2016.
- [6] H. Su, S. Maji, E. Kalogerakis, and E. Learned-Miller, “Multi-view convolutional neural networks for 3D shape recognition,” in *Proceedings of the IEEE international conference on computer vision*, 2015.
- [7] A. Kanezaki, Y. Matsushita, and Y. Nishida, “Rotationnet: Joint object categorization and pose estimation using multiviews from unsupervised viewpoints,” in *Proceedings of IEEE International Conference on Computer Vision and Pattern Recognition (CVPR)*, 2018.
- [8] S. Savarese and L. Fei-Fei, “3D generic object categorization, localization and pose estimation,” in *2007 IEEE 11th International Conference on Computer Vision*. IEEE, 2007, pp. 1–8.
- [9] K. Lai, L. Bo, X. Ren, and D. Fox, “A scalable tree-based approach for joint object and pose recognition,” in *Proceedings of the AAAI Conference on Artificial Intelligence*, 2011.
- [10] H. Zhang, T. El-Gaaly, A. Elgammal, and Z. Jiang, “Joint object and pose recognition using homeomorphic manifold analysis,” in *Proceedings of the AAAI Conference on Artificial Intelligence*, 2013.
- [11] A. Bakry and A. Elgammal, “Untangling object-view manifold for multiview recognition and pose estimation,” in *European conference on computer vision*. Springer, 2014, pp. 434–449.
- [12] A. Kuznetsova, S. J. Hwang, B. Rosenhahn, and L. Sigal, “Exploiting view-specific appearance similarities across classes for zero-shot pose prediction: A metric learning approach,” in *Proceedings of the AAAI Conference on Artificial Intelligence*, vol. 30, no. 1, 2016.
- [13] M. Elhoseiny, T. El-Gaaly, A. Bakry, and A. Elgammal, “A comparative analysis and study of multiview CNN models for joint object categorization and pose estimation,” in *International Conference on Machine learning*. PMLR, 2016, pp. 888–897.
- [14] H. Dutagaci, C. P. Cheung, and A. Godil, “A benchmark for best view selection of 3D objects,” in *Proceedings of the ACM workshop on 3D object retrieval*, 2010, pp. 45–50.
- [15] S. Kasaei, J. Sock, L. S. Lopes, A. M. Tomé, and T.-K. Kim, “Perceiving, learning, and recognizing 3d objects: An approach to cognitive service robots,” in *Proceedings of the AAAI Conference on Artificial Intelligence*, 2018.
- [16] J. Sock, S. Hamidreza Kasaei, L. Seabra Lopes, and T.-K. Kim, “Multi-view 6D object pose estimation and camera motion planning using rgbd images,” in *Proceedings of the IEEE International Conference on Computer Vision (ICCV) Workshops*, 2017.
- [17] L. Li, K. Jamieson, G. DeSalvo, A. Rostamizadeh, and A. Talwalkar, “Hyperband: A novel bandit-based approach to hyperparameter optimization,” *The Journal of Machine Learning Research*, vol. 18, no. 1, pp. 6765–6816, 2017.
- [18] J. Deng, W. Dong, R. Socher, L.-J. Li, K. Li, and L. Fei-Fei, “ImageNet: A Large-Scale Hierarchical Image Database,” in *CVPR09*, 2009.
- [19] M. Sandler, A. Howard, M. Zhu, A. Zhmoginov, and L.-C. Chen, “Mobilenetv2: Inverted residuals and linear bottlenecks,” in *Proceedings of the IEEE conference on computer vision and pattern recognition*, 2018, pp. 4510–4520.
- [20] K. Simonyan and A. Zisserman, “Very deep convolutional networks for large-scale image recognition,” *arXiv preprint arXiv:1409.1556*, 2014.